

Design, Optimization and CFD Analysis of a Split Type Free Piston Stirling Cooler for Onboard Applications

B. S. Archana, B.T. Kuzhiveli

Centre for Advanced Studies in Cryogenics
National Institute of Technology Calicut, India

ABSTRACT

A Stirling cryocooler is a device that operates on a closed thermodynamic cycle that produces a cooling effect. Stirling coolers are capable of producing cooling that ranges from milliwatts to many watts according to the need. An important application of Stirling cryocoolers is for cooling infrared sensors in satellites. A free piston Stirling cooler is a type of Stirling cooler in which the power piston is operated with the help of a linear motor.

In the initial part of this study, a novel moving-magnet-type split free-piston Stirling cryocooler of 0.5 W cooling capacity was designed and optimized with the help of SAGE 11 software. It produced a Carnot efficiency of 0.143 %. Then the effects of various input and geometric parameters were analyzed with the help of SAGE 11 software.

In the second part of the study, a 2-D model of the split type free piston Stirling cryocooler was created. Then the CFD analysis of the same was done. The dynamic mesh approach was used for incorporating the back-and-forth linear motion of the piston and displacer. The main results obtained from the simulations are presented in both tabular and graphical form.

INTRODUCTION

The usage of cooled imaging IR-based sensors in space applications is increasing day by day. For the proper working of an IR sensor, a good signal-to-noise ratio is needed. This requires that heat be continuously removed from the sensor. Stirling coolers are one of the best devices that can be used for cooling this type of sensor.

Stirling coolers are devices that work on a closed regenerative thermodynamic cycle known as the Stirling cycle. The Stirling cycle consists of two isothermal processes and two isochoric processes. Alternate compression and expansion of the working fluid in a closed space results in the required cooling effect. In most cases, helium is used as the working fluid.

Generally speaking, Stirling coolers can be categorized as either a kinematic type, where piston and displacer are mechanically linked to a common drive shaft, or as a free piston type, where piston and displacer are not constrained by a crankshaft or other mechanical transmission [1]. A Stirling cycle machine consists of two variable volume spaces (compression and expansion), each at different temperatures and physically separated by a regenerator [2].

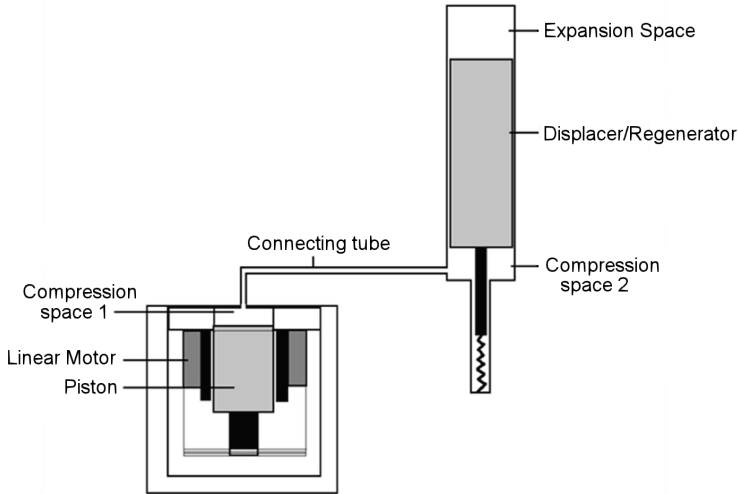


Figure 1. The schematic of the free piston Stirling cooler

In Stirling coolers, the displacer moves at the same frequency as the compressor piston, and there needs to be a proper phase difference between their motions to achieve the required cooling effect. In a free piston type of Stirling cooler, a linear motor is used to impart motion to the piston. The main components of a free piston Stirling cooler are its piston, displacer, regenerator, linear motor, etc.

Alpha, beta, and gamma (split type) are the three different configurations of Stirling coolers. The split type configuration is often preferred because it can achieve lower vibration at the IR sensor because the piston and the displacer are arranged in two separate cylinders. This is helpful to improve the signal-to-noise ratio of the IR sensor.

Stirling coolers are preferable over other coolers due to their high operating speed and pressure which directly enhance the cooling effect [3]. Park [4] used a free position Stirling cooler driven with an oil-free linear compressor that can produce a cold end temperature of 110 K. Caughey [5,6] proposed a novel concept for a free-piston Stirling cooler using a metallic diaphragm and a prototype was made. He conducted experiments as well as computational analysis with the newly proposed model.

The present study consists of two parts. In the initial part, a split type free piston cryocooler of 0.5W at 80 K was designed and optimized with the help of Sage 11 software, and some parametric analyses were conducted. In the second part, a 2-D model of the same split type Stirling cooler was created with the help of ANSYS FLUENT and a CFD analysis was conducted and compared with the earlier analyses.

DESIGN APPROACH OF THE SPLIT TYPE FREE PISTON STIRLING CRYOCOOLER

The main objective of this study was to design a split-type free piston Stirling cooler capable of producing 0.5 W of cooling effect with a cold head temperature of 80 K. The cryocooler was designed with the help of SAGE 11 software. SAGE is a one-dimensional graphical user interface for designing Stirling devices. Figure 1 shows a schematic of the free piston Stirling cooler driven by a moving magnet linear motor. The above-mentioned cryocooler was designed for a charge pressure of 15 bar and a frequency of 60 Hz. The source temperature was taken as 300 K, and the sink temperature was taken as 80 K. Helium is used as the working fluid. The input parameters of the split type free piston cryocooler are summarized in Table 1.

In this type of free piston Stirling cryocooler, the regenerator material is placed inside the displacer. Therefore, the displacer itself acts as the regenerator. A one-dimensional simulation of the cryocooler has been performed with SAGE 11 software, and the results are provided in Table 2. After the initial solution, the cryocooler was optimized, and the optimization results are given in Table 3.

Table 1. Input parameters of 0.5 W split type free piston Stirling cooler

Input parameters	Values
Compressor	
Piston length	40 mm
Piston diameter	16 mm
Piston amplitude	8 mm
Displacer	
Displacer length	50 mm
Displacer diameter	8 mm
Regenerator	
Material	SS304
Porosity	0.69
Wire diameter	0.0245 mm
Mesh no.	400
Connecting Tube	
Length	50 mm
Diameter	3.2 mm
Volumes	
Compression space1 volume	10050 mm ³
Compression space2 volume	150 mm ³
Expansion space volume	150 mm ³
Spring Stiffness	3000 N/m

Table 2. Output parameters obtained after solving

Output parameters	Values
Q _{lift}	0.5214 W
Q _{rejected}	13.38 W
W _{pv}	12.92 W
Cop actual	0.0404
Cop theoretical	0.3637
Carnot efficiency	0.1109
Displacer amplitude	1.364 mm

Table 3. Optimized parameters

Optimized parameters	Values
Q _{lift}	0.5418 W
Q _{rejected}	10.54 W
W _{pv}	10 W
Displacer spring stiffness	2284 N/m
Amplitude of constrained piston	7.6 mm
Negative facing area	29.1 mm ²
Displacer amplitude	1.912 mm
Displacer Phase angle	41.83°

Figures 2 and 3 display the effect of charge pressure on the Q_{lift} and the COP of the cryocooler. When the charge pressure increases, automatically the compression ratio associated with the given system increases, and as a result of this, the cooling load (Q_{lift}) produced by the system increases. When the charge pressure increases, the COP of the system will also increase.

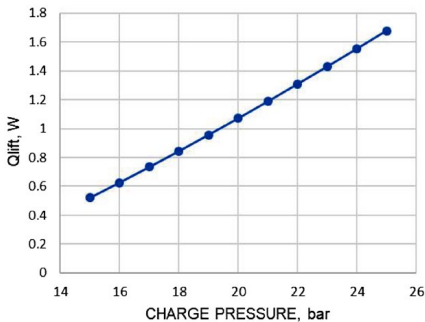


Figure 2. Effect of charge pressure on Q_{lift}

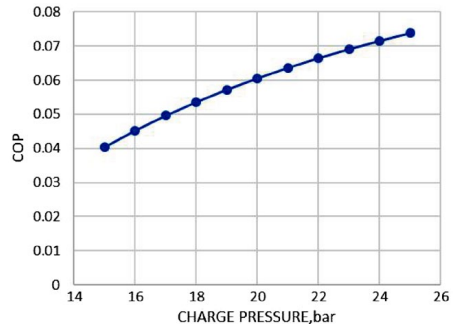


Figure 3. Effect of charge pressure on COP

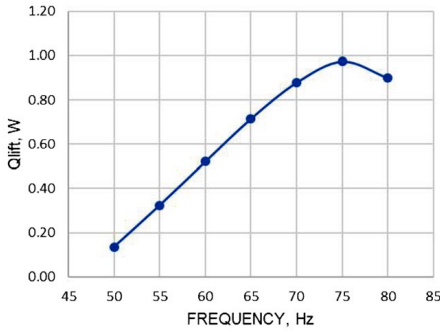


Figure 4. Effect of frequency on Q_{lift}

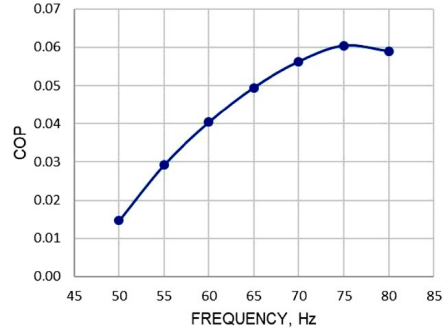


Figure 5. Effect of frequency on COP

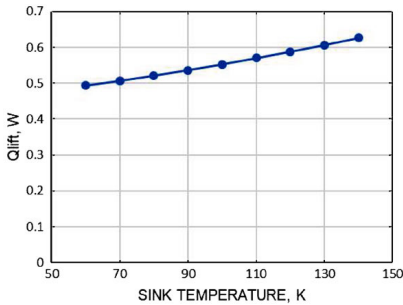


Figure 6. Effect of Sink temperature on Q_{lift}

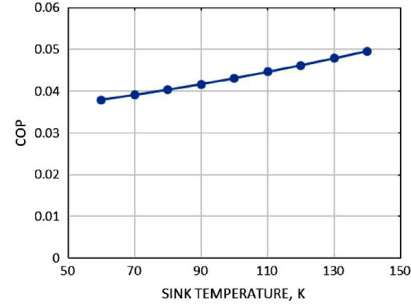


Figure 7. Effect of sink temperature on COP

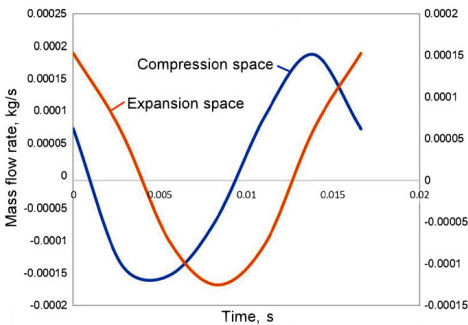


Figure 8. Variation of mass flow rate in the compression space and expansion space with time

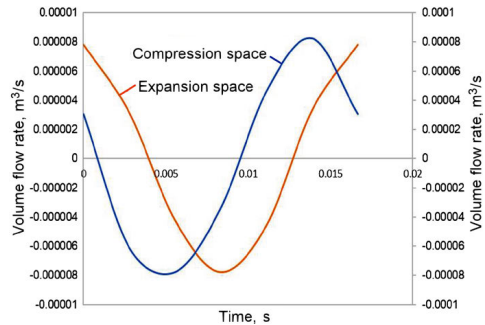


Figure 9. Variation of mass flow rate in the compression space and expansion space with time

Figures 4 and 5 represent the effect of frequency on Q_{lift} and COP of the cryocooler. For this study, the frequency was varied from 50 Hz to 80 Hz. Initially, when the frequency of the system increases the Q_{lift} of the system also increases, and it reaches an optimum point; after that it decreases. In this case, the value of the optimum frequency that gave maximum Q_{lift} was 75 Hz. The same trend can be seen with the COP vs frequency graph.

Figures 6 and 7 display the variation of cooling load and COP with sink temperature. Both COP and Q_{lift} vary linearly with an increase in sink temperature. This is because, as sink temperature increases, the amount of input work given to the cryocooler decreases.

Figures 8 and 9 show the variation of mass flow rate and volume flow rate in the compression space and expansion space with time. Here both the mass flow and volume flow rate in the expansion space lead the mass flow and volume flow rate in the compression space by a particular phase angle. In this case, the phase difference is 68.75° .

Table 4. Input parameters to REGEN 3.3

Input parameters to REGEN	Values
Gas temperature cold	80 K
Gas temperature hot	300 K
Frequency	60 Hz
Hydraulic diameter	0.0566 mm
Mass flux cold	0.0931 g/s
Average pressure	15.4 bar
Pressure ratio	1.4
Pressure phase	21°
Regenerator Area	50.2400mm ²
Regenerator Length	50 mm
Porosity	0.69
Material	Stainless Steel

Table 5. Outputs obtained from REGEN

Outputs from REGEN	Values
P-V work done by gas at the warm end (PVWKOT)	12.8 W
Adjusted net refrigeration power (NTCADJ)	0.5106 W
Coefficient of performance (NTACOP)	0.0399
Second law efficiency (EFFIC)	0.1496
Adjusted gross refrigeration power (GRCADJ)	1.216 W
Average pressure drop in regenerator (DELPVAV)	0.400 bar
Ineffectiveness (INEFCT)	0.0045
Regenerator loss (RGLOSS)	0.1542 W
Portion of enthalpy flux due to pressurization (PRLOSS)	0.0327 W
Thermal flux from matrix at right side (HTFLUX)	0.5507 W

REGENERATOR LOSS ANALYSIS OF THE CRYOCOOLER USING REGEN 3.3 SOFTWARE

In Stirling cryocoolers, a regenerative type of heat exchanger is used for transferring heat to and from the working fluid. The regenerator can be considered as the heart of a Stirling cooler. The regenerator effectiveness plays an important role in obtaining the required cooling effect in a cryocooler. In an ideal Stirling cryocooler, it is assumed that there are no losses encountered within the regenerator and it is hundred percent effective. But in the actual case, the regenerator is not one hundred percent effective; there exist some ineffectiveness due to various losses that occur in it.

$$Q_{net} = Q_{max} - Q_{losses} \quad (1)$$

$$Q_{losses} = Q_{th} + Q_{lc} + Q_{pd} \quad (2)$$

$$Q_{pd} = Q_{fp} + Q_{vp} \quad (3)$$

In a Stirling cooler, the net refrigeration effect can be represented as the difference between the refrigeration obtained from an ideal cycle (Q_{max}) to losses obtained from an actual cycle (Q_{losses}). In the above equation, Q_{th} , Q_{lc} , Q_{fp} , Q_{vp} represent the thermal conduction loss, longitudinal conduction loss, frictional pressure drop, and void volume pressure drop through the regenerator, respectively.

The regenerator design code developed by NIST is known as REGEN 3.3, and it can be used to numerically estimate the various losses encountered in the regenerator. The REGEN 3.3 model is based on a numerical solution of the one-dimensional equations for the flow of the working fluid through a porous matrix with an additional thermal conservation equation for the temperature of the matrix.

In this model, the numerical approximation is a discretization of the differential equations for conservation of mass, momentum and energy in the gas and regenerator matrix [10]. For conducting a numerical simulation using REGEN 3.3 certain input parameters are required. These are enumerated in Table 4; several of these input parameters are taken from the SAGE 11 software output.

The main outputs associated with the REGEN 3.3 simulation are shown in Table 5. These include the adjusted net refrigeration power, adjusted gross refrigeration power, P-V work done by gas at the warm end, COP, thermal losses, and various pressure losses.

The COP of the system is given by:

$$COP = NTCADJ/PVWKOT \quad (4)$$

where $NTCADJ$ is the net refrigeration power and $PVWKOT$ is the P-V work done by the gas at the warm end.

Table 6 shows a comparison of the net refrigeration effect and COP produced by the Stirling cooler from SAGE and REGEN. From the results, it is clear that there is only a small variation in the results, and the error value is in the acceptable range.

Table 6. Comparison of outputs obtained from SAGE and REGEN

	SAGE Results	REGEN Results	Error
Refrigeration effect produced	0.5214 W	0.5106 W	2.07 %
Work input	12.92 W	12.80 W	0.92 %
COP	0.0404	0.0399	1.24 %

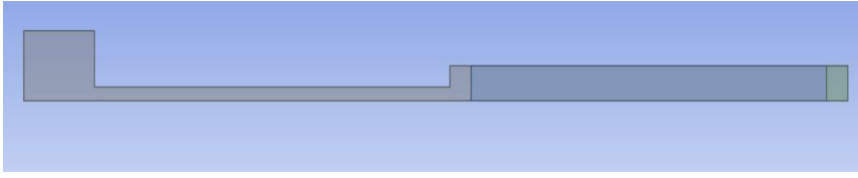


Figure 10. The geometry of split type Stirling cryocooler

CFD ANALYSIS OF THE SPLIT TYPE FREE PISTON CRYOCOOLER

By modeling the equations for particular scenarios, employing numerical solution techniques, and making a number of assumptions, CFD solves heat transfer, mass transfer, and fluid flow problems numerically. Because there are a number of inconsistencies and irrational outcomes that can arise during simulation, such as the assumption that all events will unfold as planned, the solution reached by computer modeling cannot be regarded as the optimal one. Preprocessor, solver, and post-processor are the major three processes in the CFD simulation process.

The basic governing equations used in the CFD are: conservation of mass

$$\frac{\partial \rho}{\partial t} + \nabla(\rho \vec{v}) = S_m \quad (5)$$

conservation of momentum

$$\frac{\partial}{\partial t}(\rho \vec{v}) + \nabla(\rho \vec{v} \vec{v}) = -\nabla p + \nabla \cdot (\tau) + \rho \vec{g} + \vec{F} \quad (6)$$

conservation of energy

$$\frac{\partial}{\partial t}(\rho E) + \nabla \cdot (\vec{v}(\rho E + p)) = \nabla \cdot (k_{eff} \nabla T - \sum_j h_j \vec{\phi}_j + (\tau \cdot \vec{v})) + S \quad (7)$$

In this study, a 2-D model of the cryocooler geometry has been created by using the design modular software of ANSYS. In this study, a 2-D axis-symmetric model of the cryocooler geometry has been created using the design modular software of ANSYS. Initially, the geometry was created as three different bodies: the main part, the regenerator part, and the expansion part. Then the three different bodies were converted into a single part by using the freeze option (see Figures 10).

After modeling the geometry, meshing of the geometry was carried out using the default meshing software of ANSYS. In this problem, the element for meshing was chosen as 0.08 mm and the multizone quad/tri method was used for meshing. Face meshing was also used for eliminating the skewness associated with the geometry. The number of elements and nodes created after meshing was 60876 and 62460, respectively. The resulting meshes are illustrated in Figures 11 and 12.



Figure 11. Meshed geometry Stirling cryocooler

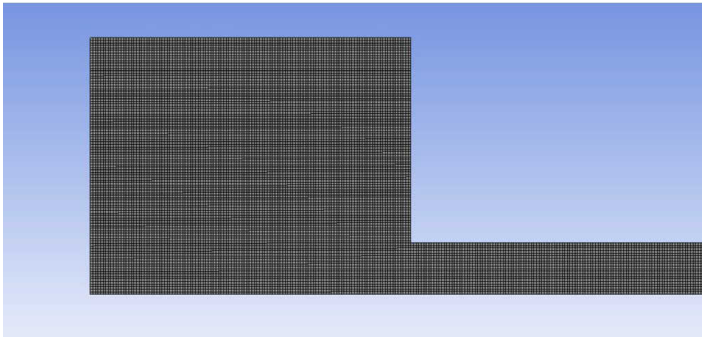


Figure 12. Enlarged view of Meshed geometry

Table 7. Details of solver

Details of solver	
Solver	Pressure Based
Time	Transient
Viscous Model	K -ε
Pressure Velocity coupling	PISO
Spacial Discretization	
Pressure	PRESTO
Momentum	Second order upwind
Energy	Second order upwind
Dynamic mesh	Layering
Boundary condition	
Piston_wall	SS, Adiabatic
Connecting tube	SS , Isothermal
Regenerator	SS, Porous media
Viscous resistance of regenerator	2.41E+10
Inertial resistance of regenerator	76050
Expansion Space	SS, Adiabatic
Cold_tip	SS Adiabatic

The piston and the displacer are continuously moving in a Stirling cooler, so one needs to use the dynamic mesh concept for incorporating the motion of elements near the piston and the displacer. The dynamic mesh model in ANSYS fluent offers flow modeling of a material region whose boundaries are changing with respect to time [7].

Basically, there are three different types of dynamic meshing methods associated with ANSYS fluent: they are the smoothing, layering and local re meshing techniques. For this problem we have chosen the layering technique. Since the piston and the displacer of the cryocooler are moving, we need to give a motion profile for the piston and the displacer. We get from the SAGE 11 software the stroke of the displacer and the phase angle between the piston and the displacer. A Mat lab code was written with the stroke of the piston and the displacer, and the phase difference and the frequency of the cryocooler. Then this profile was given to the piston and displacer in ANSYS fluent while doing the dynamic meshing.

$$V_p = X_p \omega \text{ Cos}(\omega t) \tag{8}$$

$$V_d = X_d \omega \text{ Cos}(\omega t + \Phi) \tag{9}$$

Here X_p and X_d represent the displacement of piston and displacer, respectively, and V_p and V_d represent the velocity of the piston and displacer, respectively. ω is the angular frequency, and Φ is the phase difference between the piston and displacer. The various input parameters and the boundary conditions used in the ANSYS fluent model are given in Table 7.

Figure 13 represents the pressure contours of the Stirling cooler. From the figure it can be seen that the pressure along the length of the cooler is decreasing. Figures 14 and 15 illustrate the velocity contours and velocity magnitudes within the Stirling cooler, respectively. From the velocity contours its can be seen that the flow through the regenerator is very negligible.

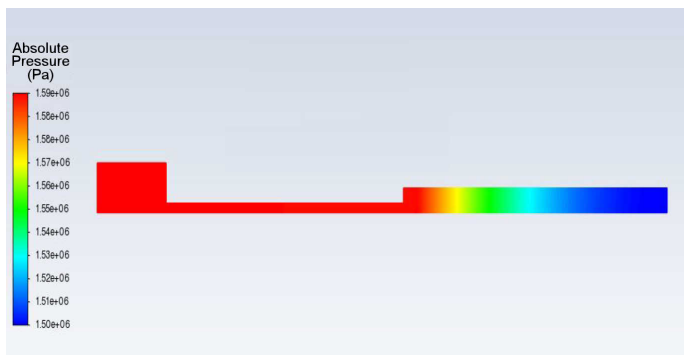


Figure 13. Pressure contour of Stirling cooler

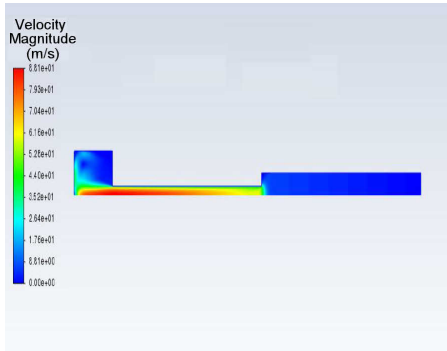


Figure 14. Velocity contour of Stirling cooler

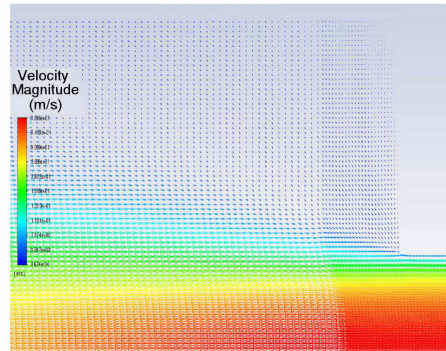


Figure 15. Velocity magnitude of Stirling cooler

CONCLUSION

As a first step in this work, a split type free piston Stirling cryocooler of 0.5 W at 80 K was designed and optimized with the help of SAGE 11 software. Next, the effects of different operating parameters were analyzed to determine their effect on the cooling load (Q_{lift}) and COP.

The various losses occurring within the regenerator were then determined using REGEN 3.3 software, and the cooling load and COP as obtained from SAGE 11 and REGEN 3.3 software were compared.

In the second part of the work, a 2-D axis-symmetric model of the split type free piston Stirling cryocooler was created using ANSYS fluent software which incorporated various input and output parameters from the SAGE 11 software and the CFD analysis.

REFERENCES

1. Shunmin Zhu, Guoyao Yu, Xiaowei Li, Wei Dai and Ercang Luo, "Parametric study of a free-piston Stirling cryocooler capable of providing 350 W cooling power at 80 K," *Applied Thermal Engineering*, 174 (2020).
2. Muluken Zegeye Getie, François Lanzetta, Sylvie Bégot, Bimrew T. Admassu, Abdulkadir A. Hassenc, "Reversed regenerative Stirling cycle machine for refrigeration application: A review," *International Journal of Refrigeration*, 118 (2020), pp. 173-187.
3. Fayaz H. Kharadi, A. Karthikeyan and Bhojwani Virendra, "40 K single-stage split-type Stirling cryocooler," *International Journal of Ambient Energy* (2019).
4. P. Jiho, I. Sehwan, K. Junseok, K. Hyobong, H. Yongju, Y. Hankil and P. Seongje, "Development and parametric study of 1 kW class free-piston Stirling cryocooler driven by a dual opposed liner compressor for LNG (Re) liquefaction," *International Journal of refrigeration*, 104 (2019), pp. 113-122.
5. C. Alan, S. Mathieu, G. Michael and T. Alan, "A free-piston Stirling cooler using metal diaphragm," *Cryogenics*. 80 (2016), pp. 8-16.
6. Alan Caughley, Mathieu Sellier, Michael Gschwendtner, Alan Tucker, "CFD analysis of a diaphragm free-piston Stirling cryocooler," *Cryogenics*, 79 (2016), pp. 7-16.
7. K.Q.Luo, Y.L. Sun, Z .J. Jiang, E.C.Luo, J.Y. H u, L.M. Zhang, Z .H .Wu, Z.L.Jia and Y. Zhou, "A Free-Piston Stirling Cooling Prototype for Ultra-Low Temperature Freezing," *Cryocoolers 21*, ICC Press, Boulder, CO (2021), pp. 215-220.
8. Ruijie Li and Lavinia Grosu., "Parameter effect analysis for a Stirling cryocooler," *International journal of Refrigeration*. 80, (2017), pp. 92-105.
9. D. Gedeon, *Sage User's Guide Stirling, Pulse-Tube and Low-T Cooler Model Classes* (2016).
10. J. Gary, A.O. Gallagher, R. Radebaugh, Y. Huang, and E. Marquardt, *REGEN 3.3 User Manual*, NIST (2008).